

# VIBRATION INSENSITIVE INTERFEROMETRY

James Millerd, Neal Brock, John Hayes, Brad Kimbrough, Michael North-Morris,  
and James C. Wyant<sup>(1)</sup>

4D Technology Corporation, 3280 Hemisphere Loop, Suite 146, Tucson, AZ 85706

<sup>(1)</sup>College of Optical Sciences, University of Arizona, Tucson, AZ 85721

<http://www.optics.arizona.edu/jcwyant>

[jcwyant@optics.arizona.edu](mailto:jcwyant@optics.arizona.edu)

## ABSTRACT

The largest limitation of phase-shifting interferometry for optical testing is the sensitivity to the environment, both vibration and air turbulence. An interferometer using temporal phase-shifting is very sensitive to vibration because the various phase shifted frames of interferometric data are taken at different times and vibration causes the phase shifts between the data frames to be different from what is desired. Vibration effects can be reduced by taking all the phase shifted frames simultaneously and turbulence effects can be reduced by averaging many measurements. There are several techniques for simultaneously obtaining several phase-shifted interferograms and this paper will discuss two such techniques: 1) Simultaneous phase-shifting interferometry on a single detector array (PhaseCam) and 2) Micropolarizer phase-shifting array. The application of these techniques for the testing of large optical components, measurement of vibrational modes, the phasing of segmented optical components, and the measurement of deformations of large diffuse structures is described.

## 1. INTRODUCTION

Phase-shifting interferometry has proven to be extremely useful for the testing of optics, but in many situations, especially for the testing of large telescope optics, the measurement accuracy is limited by the environment and sometimes the environment is sufficiently bad that the measurement cannot be performed. This paper describes advances in reducing effects of vibration by using dynamic interferometry techniques. If the interferometer is insensitive to vibration many measurements can be averaged to reduce the effects of air turbulence and large optical components can be tested, segmented optical components can be phased, and deformations of large diffuse structures can be measured.

## 2. SIMULTANEOUS PHASE-SHIFTING INTERFEROMETER

In conventional phase-shifting interferometry, 3 or more interferograms are obtained where the phase difference between the two interfering beams changes by 90-degrees between consecutive interferograms [1]. An interferometer using temporal phase-shifting is very sensitive to vibration because the various phase shifted frames of interferometric data are taken at different times and vibration causes the phase shifts between the data frames to be different from what is desired. Vibration effects can be reduced if all the phase shifted frames are taken simultaneously. Figure 1 shows a convenient way to obtain four phase-shifted interferograms on a single CCD camera [2, 3].

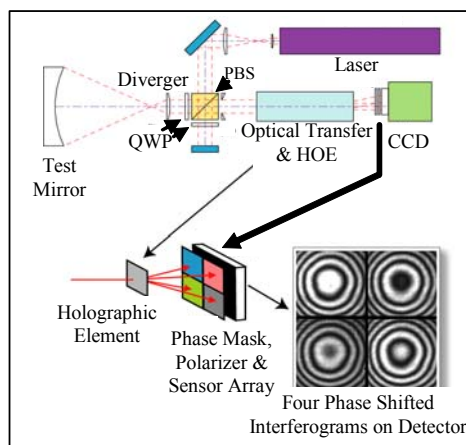


Fig. 1. Simultaneous phase-shifting interferometer (PhaseCam).

In this arrangement an interferometer is used where a polarization beamsplitter causes the reference and test beams to have orthogonal polarization. Quarter-wave plates are placed in the reference and test beams so the beam transmitted the first time through the beamsplitter is reflected the second time, and vice versa. After the two orthogonally polarized beams are combined they pass through a holographic element that splits the beam into four separate beams resulting in

four interferograms. These four beams pass through a birefringent mask that is placed just in front of the camera. The four segments of the birefringent mask introduce phase shifts between the test and reference beams of 0, 90, 180, and 270 degrees. A polarizer with its transmission axis at 45 degrees to the direction of the polarization of the test and reference beams is placed after the phase masks just before the CCD array. Thus, all four phase-shifted interferograms are detected simultaneously on a single detector array. While it is necessary to determine the corresponding detector elements for the four interferograms, once this alignment information is determined it is constant with time.

By making short exposures the vibration, as well as the air turbulence is frozen. The effects of air turbulence can be reduced by taking many sets of data, where the time between the different data sets is long compared to the time it takes for the turbulence to change, and then averaging the data.

In phase-shifting interferometry errors having twice the frequency of the interference fringes are commonly obtained if the phase shifts are not exactly 90 degrees [1]. These double frequency errors are also present in simultaneous interferometers, but they can be greatly reduced if several frames of data are taken with the average phase difference between the two interfering beams different for each frame. That is, a simultaneous phase shifting interferometer will actually give more accurate measurements if vibration is present and several data frames are averaged than if no vibration is present. Double frequency phase measurement errors can nearly be eliminated in a simultaneous phase-shifting interferometer. This is a large advantage of simultaneous phase-shifting interferometers.

### 3. MICROPOLARIZER PHASE-SHIFTING ARRAY

The above technique for simultaneous phase-shifting is great if a single wavelength is used, but due to dispersion in the HOE it does not work well for white light interferometry or multiple wavelength techniques that are especially useful for the phasing of mirror segments. Another technique that does work well with multiple wavelengths or white light because the phase shift between the two interfering beams is nearly independent of wavelength is a quarter waveplate followed by linear polarizers at different angles. The quarter waveplate is oriented to convert the test beam into left-handed circular polarization and the reference beam into right-handed circular polarization. It can be shown [4] that if these circularly polarized beams are transmitted through a linear polarizer a phase shift

between the two interfering beams proportional to twice the rotation angle of the polarizer results.

Let the test beam be left circularly polarized with a phase of  $\delta_t$ , and the reference beam be right circularly polarized with a phase of  $\delta_r$ . Further, let both beams be incident upon a linear polarizer oriented at an angle  $\alpha$  with respect to the x-axis. Upon passing through the polarizer, both the test and reference beams are now linearly polarized at an angle  $\alpha$  and a phase offset of  $+\alpha$  has been added to the test beam, whereas a phase offset of  $-\alpha$  has been added to the reference beam. The two beams are now collinear and will interfere to give an intensity pattern in accordance with

$$I(x, y) = I_t(x, y) + I_r(x, y) + 2\sqrt{I_t I_r} \cos[\Delta\phi(x, y) + 2\alpha] \quad (1)$$

where  $I_t$  and  $I_r$  are the intensities of the test and reference beams,  $\Delta\phi = \delta_t - \delta_r$  is the phase being measured, and  $2\alpha$  is the phase shift. The linear polarizer acts as a phase shifting device between the two beams, where the phase shift is equal to twice the orientation angle of the polarizer as illustrated in Figure 2.

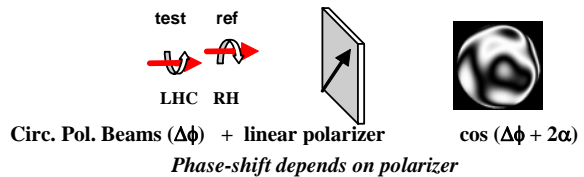


Figure 2. Use of polarizer to introduce phase shift between test and reference beams.

Thus, if a phase mask is made of an array of 4 linear polarizer elements having their transmission axes at 0, 45, 90, and -45 degrees as shown in Figure 3a, where a polarizer element is placed over each detector element, the mask will produce an array of four 0,  $\pi/2$ ,  $\pi$ , and  $-\pi/2$  degrees phase shifted interferograms. Likewise, a phase mask can be made using an array of 4 linear polarizer elements having their transmission axes at 0, 45, -45 and 90 degrees as shown in Figure 3b.

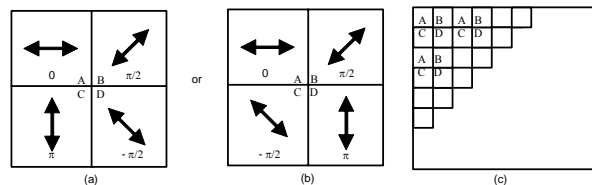


Figure 3. Phase filter. (a) 4 polarizer elements giving 0, 90, 180, and -90 degree phase shifts. (b) 4 polarizer elements giving 0, 90, -90, and 180 degree phase shifts. (c) Phase filter made up of array of 4 polarizer elements.

While an achromatic quarter waveplate could be used to extend the spectral range the phase mask would work for, it turns out that the phase shift produced by the rotated polarizers does not depend greatly upon the quarter-wave plate being a true quarter-waveplate [5, 6]. A phase shifter of this type is often called a geometrical phase shifter since the phase shift is independent of wavelength. Having a phase shift independent of wavelength is important in multiple wavelength or white light interferometers.

The phase distribution can be calculated using a 2 x 2 element array, or in many cases the errors can be further reduced by using a 3 x 3 element array as shown in Figure 4.

0	$\frac{\pi}{2}$	0	$\frac{\pi}{2}$			
$-\frac{\pi}{2}$	1	$\pi$	2	$-\frac{\pi}{2}$	3	$\pi$
0	4	$\frac{\pi}{2}$	5	0	6	$\frac{\pi}{2}$
$-\frac{\pi}{2}$	7	$\pi$	8	$-\frac{\pi}{2}$	9	$\pi$

Figure 4. Calculation of phase using 3 x 3 element array.

In this case the tangent of the phase for element 5 is given by

$$\tan[\theta_5] = \frac{2(I_2 + I_8 - I_4 - I_6)}{-I_1 - I_3 + 4I_5 - I_7 - I_9} \quad (2)$$

Figure 5 shows a schematic of a Twyman-Green interferometer using the micropolarizer phase-shifting array. The essential characteristics of the two-beam interferometer is that the test and reference beams have orthogonal polarization and the micropolarizer array matches the CCD array.

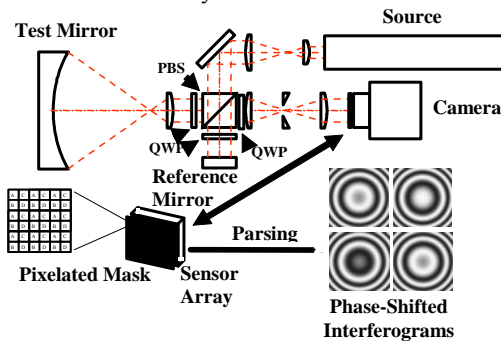


Figure 5. Interferometer Configuration

#### 4. SINGLE SHOT LASER-BASED FIZEAU INTERFEROMETER

It is harder to make a single shot laser-based Fizeau interferometer than a Twyman-Green interferometer because the Fizeau is more common path and it is hard to obtain a reference and test beam having orthogonal polarization. In principle a quarter-wave plate can be placed between the test and reference surfaces to rotate the direction of polarization of the test beam by 90 degrees, but in practice this does not work well, especially for the testing of spherical optics. Techniques where the reference and test beams are tilted with respect to each other have been described [7], but a better approach is the on-axis approach shown below [7].

In this approach, a short coherence light source is used. The source beam consists of two time delayed orthogonally polarized beams. The time delay (path difference) between the two beams is set equal to the path delay in the Fizeau cavity. The desired interference results from the long path source beam reflected off the reference surface and the short path length source beam reflected off the test surface. All beams are on-axis so off-axis aberrations are not a problem. Since both source beams are reflected off both test and reference surfaces and only the two path-length matched beams give interference the fringe contrast is reduced, but it is still more than adequate. Because a short coherence light source is used spurious fringes are greatly reduced. One source that works well is a modulated diode having a coherence length of approximately 300 microns.

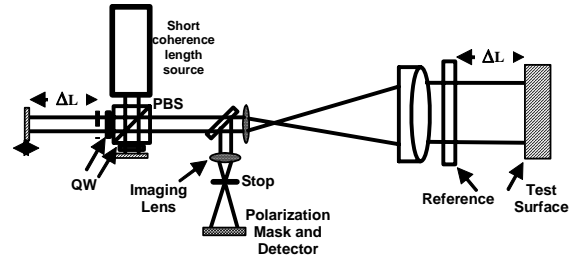


Figure 6. Simultaneous phase-shifting Fizeau – short coherence length source.

#### 5. APPLICATIONS

Several applications of a vibration insensitive (dynamic interferometer) are shown below.

##### 5.1 Testing of large optics

Figure 7 shows typical grey scale contour and 3D map obtained using the micropolarizer phase shifting

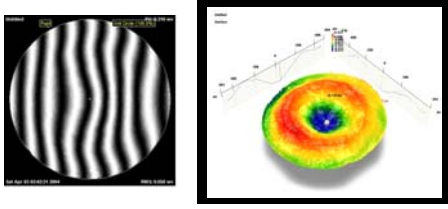


Figure 7. Measurement of 300 mm diameter, 2 meter ROC mirror. Mirror and interferometer on separate tables.

interferometer in the presence of vibration. For this example the test mirror and interferometer were placed on separate tables and no vibration isolation was present. RMS measurement repeatability is determined by the air turbulence and is typically a few nm. The effects of air turbulence can be reduced by averaging and the rms error due to air turbulence typically reduces by the square root of the number of data frames averaged.

### 5.2 Measurement of vibrational modes

Not only can the effects of vibration be eliminated, but by making short exposures to freeze the vibration the vibrational modes can be measured. Figure 8 shows an example of measuring vibration of a disk driven at a frequency of 408 Hz. Movies can be made showing the vibration.

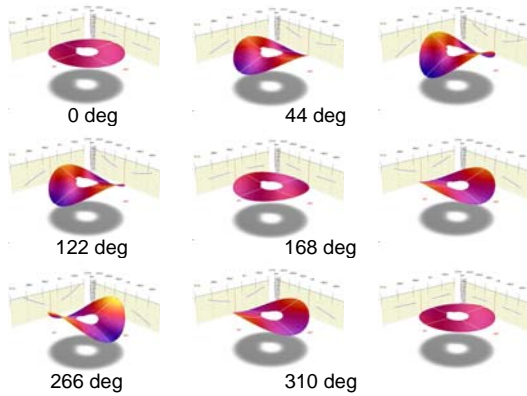


Fig. 8. Measurement of vibration of a disk (408 Hz).

### 5.3 Multi-wavelength dynamic interferometer

The benefits of using two-wavelength measurements to extend the dynamic range of an interferometric measurement are well known [8, 9]. The testing of a segmented primary telescope mirror requires the measurement of potentially large step discontinuities

between segments (millimeters) and at the same time requires high resolution (nanometers) to verify surface figure of the elements. In addition, the difficulty of vibrationally isolating large meter-class optics requires a measurement technique that is highly immune to vibration. The achromatic micropolarizer phase-shifting interferometer described above is nearly ideal for the phasing of segmented primary telescope mirrors [10].

Synthetic-wavelength measurements are made by capturing two measurements at different wavelengths and subtracting the phase. The measured difference in surface height is given by

$$\Delta opd = 2\Delta z = \frac{\Delta\phi_e}{2\pi} \lambda_e \quad \lambda_e = \frac{\lambda_1 \lambda_2}{|\lambda_1 - \lambda_2|}$$

$$\Delta\phi_e = \Delta\phi_1 - \Delta\phi_2 \quad (3)$$

The phase subtraction can be made directly by subtracting phases as shown above or it can be calculated directly from the measured intensities, facilitating the ability to measure diffuse as well as specular surfaces. The algorithm for the interferogram subtraction can be derived by applying the following trigonometric identity to the phase subtraction.

$$\tan(a-b) = \frac{\tan(a) - \tan(b)}{1 + \tan(a) \cdot \tan(b)} \quad (4)$$

$$\Delta\phi_e = \text{ArcTan}\left(\frac{X(x,y)}{Y(x,y)}\right)$$

where

$$X(x,y) = [D_1(x,y) - B_1(x,y)] \cdot [A_2(x,y) - C_2(x,y)] - [A_1(x,y) - C_1(x,y)] \cdot [D_2(x,y) - B_2(x,y)]$$

$$Y(x,y) = [A_2(x,y) - C_2(x,y)] \cdot [A_1(x,y) - C_1(x,y)] + [D_1(x,y) - B_1(x,y)] \cdot [D_2(x,y) - B_2(x,y)]$$

$A_1, B_1, C_1, D_1$  are the phase-shifted interferograms at  $\lambda_1$  and  $A_2, B_2, C_2, D_2$  are the phase-shifted interferograms at  $\lambda_2$ .

The useable synthetic wavelength range of the multi-wavelength interferometer is governed by the source wavelengths available and the uncertainty of determining the relative wavelengths. The sensitivity to wavelength uncertainty increases with synthetic wavelength. A long wavelength, such as 10 mm, is needed initially because the segments may be a long distance from being phased. It is clear that the accuracy of a single measurement using a synthetic wavelength of 10 mm is not sufficient to measure the height of a discontinuity down to the nanometer level. It takes a series of measurements at different synthetic wavelengths to achieve accuracies of a few nanometers. Measurements at longer synthetic

wavelengths are used to correct the modulo  $2\pi$  phase ambiguities at shorter wavelengths. By choosing the appropriate wavelengths it is possible to correct the phase ambiguities all the way down to the fundamental wavelength thus providing the accuracy of a single wavelength measurement.

Figure 9 shows a diagram of the source module. The broadest range of synthetic wavelengths is produced by using the fundamental source and the (tunable laser source) TLS which overlap in wavelength. The upper end of the synthetic wavelength range is limited to 10 mm by the uncertainty of the source wavelengths. The lower end of the range is limited to 115 microns due to the wavelength range of the tunable source (5nm). There is a region between 3mm and 7mm in synthetic wavelength that requires the TLS to tune over a range too large for the accurate piezo-electric transducer and the wavelength uncertainty of course tuning the DC motor becomes large. This small range of synthetic wavelength is not recommended for operation; however, this does not present a serious limitation for most practical situations. The third laser source (fixed 660nm) was added to help bridge the gap between the lowest tunable synthetic wavelength and the fundamental wavelength. Combining measurements made with the two fixed sources it is possible to measure at a synthetic wavelength of approximately 18 microns. Without this intermediate step the synthetic wavelength measurements would require an accuracy of approximately 1/1000th of a wave to reliably correct the phase ambiguities at the fundamental wavelength. Adding the 18 micron synthetic wavelength reduces the required accuracy to approximately 1/60th of a wave.

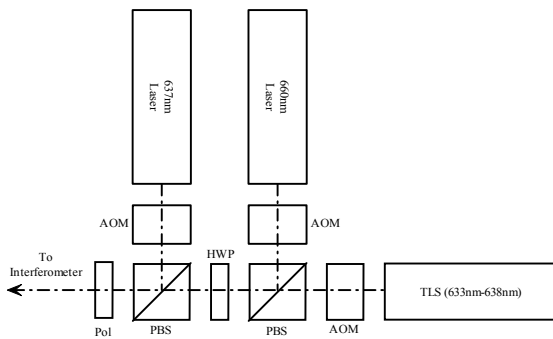


Figure 9. Three sources.

Figure 10 shows the phasing of a segmented parabolic mirror. The step between the two halves of the mirror was measured using a multi-wavelength interferometer and a micrometer.

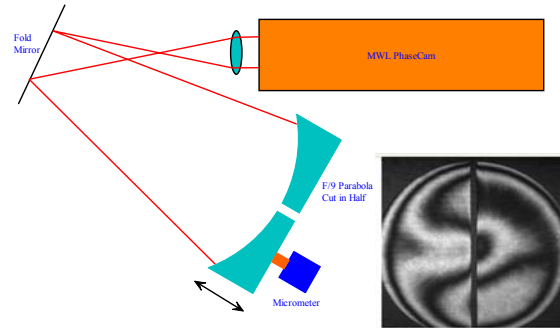


Figure 10. Measurements of Two Separated Halves of a Parabola Were Used to Correlate Step Height Measurements With a Micrometer

The estimated error in the measurement is approximately 1/100 the synthetic wavelength.

#### 5.4 Electronic speckle pattern interferometry (ESPI)

The technique for measuring changes in diffuse surfaces using Electronic Speckle Pattern Interferometry (ESPI) is well known. The single-frame spatial phase-shifting technique described above can significantly reduce sensitivity to vibration and enable complete data acquisition in a single laser pulse. The interferometer described below was specifically designed to measure the stability of the James Webb Space Telescope (JWST) backplane [11]. During each measurement the laser is pulsed once and four phase-shifted interferograms are captured in a single image. The signal is integrated over the 9ns pulse which is over six orders of magnitude shorter than the acquisition time for conventional interferometers. Consequently, the measurements do not suffer from the fringe contrast reduction and measurement errors that plague temporal phase-shifting interferometers in the presence of vibration.

The testing of the back-plane stability for primary telescope mirrors requires the measurement of large diffuse meter-class structures from a significant standoff location in the presence of vibration. Distance measuring interferometers are capable of measuring the surface deformation in one direction at discrete locations. However, the data is sparse and the technique requires attaching retro-reflectors to the structure under test which may distort the results. A better approach is to use Electronic Speckle Pattern Interferometry (ESPI). ESPI can measure the deformations of the entire surface simultaneously without attaching auxiliary optics to the test article [12]. Although, combined with traditional phase-shifting techniques a speckle interferometer can make

high resolution measurements [13], the acquisition time is too slow to provide vibration immunity. The speckle interferometer presented here combines the ability to measure large diffuse structures with spatial phase shifting to overcome the speed limitations of traditional phase-shifting interferometry. The system is capable of measuring meter-class structures with an acquisition time of 9 ns which is six orders of magnitude shorter than the acquisition time for conventional interferometers.

Phase-shifted ESPI measurements are made by capturing two measurements one before and one after the surface is perturbed and subtracting the phase. The phase subtraction can be done directly in the phase domain; however, performing the subtraction using the measured intensities as shown in Eq. 4 has the distinct advantage of facilitating the application of smoothing routines to reduce the sensitivity to random irradiance fluctuations. Although, the subtracting of two measurements significantly reduces the random irradiance pattern and enables the detection of correlation fringes, there is some speckle decorrelation between the frames resulting in fringes that are low contrast and noisy.

When considering the desired speckle size at the camera there are two competing factors that govern the selection; 1) throughput and 2) speckle decorrelation between the spatially offset pixels. The small spatial offset between the pixels used to calculate the phase leads to a difference in irradiance and phase between neighboring pixels. The larger the average speckle size relative to the offset in the pixels the smaller the differences. The obvious solution is to stop down the imaging aperture to enlarge the speckle size; however, doing so has the adverse consequence of reducing the throughput of the imaging train. When measuring large structures light is at a premium and needs to be conserved whenever possible. A good compromise between these two competing factors is to match the mean speckle size to the “unit cell” (The extent of the repeating pattern in the mask.) At this condition there is only a slight increase in the noise in the measurement for low fringe densities when compared to an extremely stable temporal phase-shifting measurement and there is practically no difference for higher fringe densities (0.2 fringes per pixel or greater.) [14]. It should be noted that in the presence of vibration the noise in the temporally phase-shifted measurement would far exceed the spatial phase-shifted measurement.

Figure 11 shows a diagram of the SpeckleCam and the actual instrument is shown in Figure 12.

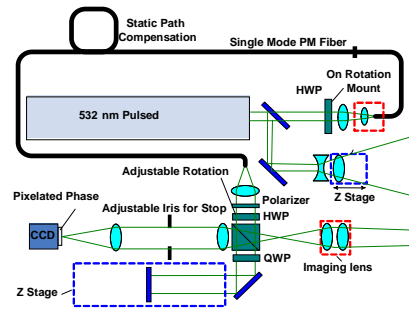


Figure 11. SpeckleCam System Layout.



Figure 12. SpeckleCam.

The operation of the interferometer was tested by measuring a 1 meter diameter target made of carbon fiber. The sample was illuminated and imaged off-axis with an angle of 5 degrees between the laser and the receiver. The interferometer and the test article were placed on separate unisolated tables with a 4m standoff between the interferometer and the target. The test article was perturbed between measurements by pushing the center of the carbon fiber target toward the interferometer with a micrometer. The resulting phase for an average of 15 measurements is shown in figure 13.

The results clearly show that a dynamic phase-shifting electronic speckle pattern interferometer that uses a single frame spatial phase-shifting technique to significantly reduce sensitivity to vibration and enable the use of a high power pulsed laser can measure deformations of large objects. The interferometer designed to measure the stability of the James Webb Space Telescope (JWST) backplane has a total acquisition time of 9 ns and enough energy in the

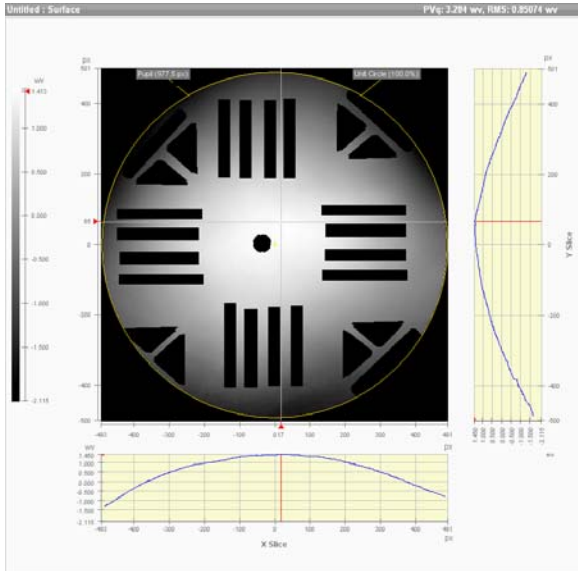


Figure 13. Surface change obtained from measurement of a 1m carbon fiber target.

illumination to measure meter-class structures. The ability to measure meter-class structures in the presence of vibration was demonstrated by measuring a 1 meter diameter carbon fiber target at a stand-off of 4 meters with the interferometer and the test article placed on different unisolated tables.

## 6. CONCLUSIONS

A single shot interferometer, can go a long way in reducing the effects of what is often the largest source of error in phase shifting interferometry, namely vibration. Errors due to air turbulence can be reduced by averaging many frames of data obtained using a single shot interferometer. Averaging data frames in the presence of vibration will average out the double frequency errors common in phase-shifting interferometry and generally more accurate results can be obtained in the presence of vibration than can normally be obtained using conventional temporal phase-shifting interferometry in the absence of vibration. Also, it is possible to measure a vibrating surface to determine precisely how the surface is vibrating. Single shot interferometry is excellent for performing multiple wavelength measurements and electronic speckle pattern interferometry. Both Twyman-Green and Fizeau interferometers can be single-shot dynamic interferometers. Once a person works with a simultaneous phase-shifting interferometer it is hard to go back to working with a temporal phase-shifting interferometer.

## 7. REFERENCES

1. Creath, K., "Phase measurement interferometry techniques," *Progress in Optics*. **26** 349-393 (1988).
2. James E. Millerd and Neal J. Brock, "Methods and apparatus for splitting, imaging, and measuring wavefronts in interferometry," U. S. Patent 6,304,330 (2001).
3. James C. Wyant, *Optics & Photonics News*, **14**, 4, 36-41 (2003).
4. James Millerd, Neal Brock, John Hayes, Brad Kimbrough, Matt Novak, Michael North-Morris and James C. Wyant, "Modern approaches in phase measuring metrology," *Proc. SPIE*, **5856**, (2005).
5. S. Suja Helen, M.P. Kothiyal, and R.S. Sirohi, "Achromatic phase-shifting by a rotating polarizer", *Opt. Comm.* **154**, 249 (1998).
6. Millerd, J.E., Brock, N.J., Hayes, J.B., North-Morris, M.B., Novak, M., and Wyant, J.C., "Pixelated phase-mask dynamic interferometer," *Proc. SPIE*, **5531**, 304-314, (2004).
7. Neal Brock, John Hayes, Brad Kimbrough, James Millerd, Michael North-Morris, Matt Novak and James C. Wyant, "Dynamic Interferometry," *Proc. SPIE* **5875**, 58750F-1, (2005).
8. Katherine Creath, Yeou-Yen Cheng, and James C. Wyant, "Contouring aspheric surfaces using two-wavelength phase-shifting interferometry," *Optica Acta*, **32**, 1455, (1985).
9. Y.-Y. Cheng and J.C. Wyant, "Multiple-Wavelength Phase-Shifting Interferometry" *Applied Optics* Vol. **24**, No. 6, pp. 804-807, 1985.
10. Michael B. North-Morris, James E. Millerd, Neal J. Brock and John B. Hayes, "Phase-Shifting Multi-Wavelength Dynamic Interferometer," *Proc. SPIE* **5531**, 64-75, (2004).
11. Michael North Morris, James Millerd, Neal Brock, John Hayes and Babak Saif, "Dynamic Phase-Shifting Electronic Speckle Pattern Interferometer," *Proc. SPIE* **5869**, 58691B-1, (2005).
12. S. Nakadate, T. Yatagai, and H. Saito, "Electronic speckle pattern interferometry using digital image processing techniques," *Applied Optics* Vol. **19**, No. 11, p. 1879-1883, 1980.
13. K. Creath, "Phase-shifting speckle interferometry," *Applied Optics* Vol. **24**, No. 18, p. 3053-3058, 1985.
14. J. Burke, H. Helmers, "Spatial versus temporal phase shifting in electronic speckle-pattern interferometry: noise comparison in phase maps," *Applied Optics*, Vol. **39**, No. 25, p. 4598-4606, 2000.